

---

## CONTRIBUTED PAPERS

---

# X-RAY DIFFRACTION CHARACTERIZATION OF MULTILAYER EPITAXIAL THIN FILMS DEPOSITED ON (0001) SAPPHIRE

THOMAS N. BLANTON AND LIANG-SUN HUNG

Imaging Research and Advanced Development, Eastman Kodak Company, Kodak Park B49, Rochester, NY 14652-3712, USA

Multilayer thin film structured components comprised of LiTaO<sub>3</sub>/MgO/Pt (lithium tantalate/magnesium oxide/platinum) have been deposited onto (0001)  $\alpha$ -Al<sub>2</sub>O<sub>3</sub> (corundum aluminum oxide or sapphire) single crystal wafers. Conventional  $\theta/2\theta$  scans and diffractometer rocking curves revealed the presence of (0001) LiTaO<sub>3</sub>/(111) MgO/(111) Pt planar alignment for the three films respectively. Pole figure analysis provided in-plane alignment results which indicate that all films are epitaxial but each show high levels of twinning. Using [1100] as the reference orientation direction for sapphire, the parallel orientation direction of each thin film was found to be [1100] LiTaO<sub>3</sub>/[110] MgO/[110] Pt.

## Introduction

Lithium tantalate (LiTaO<sub>3</sub>) and lithium niobate (LiNbO<sub>3</sub>) are desirable materials for integrated-optic applications due to their nonlinear optical properties and large electro-optic and piezoelectric coefficients [1, 2]. These phases are isostructural with trigonal space group symmetry R3c [3] but are usually indexed based on a hexagonal unit cell. Bulk single-crystal properties are well known for these materials and their usefulness could be expanded by exploitation of unique features of thin films. In the waveguide second-harmonic generation (SHG) application, the use of non-linear optical thin-film waveguides appears to be a particularly attractive approach to generating blue or green laser light for optical storage applications. Large refractive index differences achievable with thin films can lead to tighter mode confinement, and thus higher second-harmonic conversion efficiency [4]. Due to its superior resistance to laser-induced optical damage LiTaO<sub>3</sub> may be a more attractive material than LiNbO<sub>3</sub>, for thin film applications requiring high levels of laser power such as SHG [5]. Thin-film waveguides also offer advantages in available substrate size and cost. Furthermore, the thin-film approach gives the possibility of an alternate utility of the substrate. For example, an epitaxial thin film of LiTaO<sub>3</sub> in the desirable c-axis orientation has been reported on an epitaxial buffer layer of (111) MgO on a (111) GaAs substrate [6]. This epitaxial

growth makes possible the development of an integrated optic device in which sources, detectors, electronics, and nonlinear optical waveguides may be produced on a single substrate [4]. In an effort to move closer to producing such a monolithic device, we have developed thin film deposition capabilities which allow multilayer thin-film epitaxial growth of LiTaO<sub>3</sub> (nonlinear optic device) deposited on MgO (buffer layer) deposited on Pt (conductive device) deposited on (0001)  $\alpha$ -Al<sub>2</sub>O<sub>3</sub> (single-crystal sapphire substrate).

Knowledge of the microstructure of thin films is important not only for understanding what deposition conditions provide optimum property films, but it is also important for being able to reproducibly manufacture these optimized films on a microelectronic device production line. Several techniques are applied for this microstructure characterization including scanning electron microscopy (SEM), atomic force microscopy (AFM), Rutherford backscattering spectroscopy (RBS), secondary ion mass spectroscopy (SIMS), micro Raman spectroscopy ( $\mu$ RS), X-ray photoelectron spectroscopy (XPS), and X-ray diffraction (XRD). XRD is common to many laboratories, and for most thin film samples deposited on flat substrates the sample preparation and analysis is nondestructive. Conventional XRD methods (Bragg-Brentano, grazing incidence) can provide information regarding crystallinity, phase identification, and

qualitative assessment of planar orientation. Planar orientation can be quantitated using X-ray rocking curve analysis (omega scan). An enhancement of orientation understanding can be obtained if X-ray pole figure analysis is utilized. Specifically, in-plane orientation can be evaluated using the pole figure technique.

When thin films are deposited on single-crystal substrates, in-plane alignment is an important microstructural property. If the thin film in-plane alignment can be matched to a single crystallographic direction of the substrate, the film is said to be epitaxially grown. Quite often, films show alignment along one substrate crystallographic direction as well as 180 degrees rotated from this direction. Such films are said to be epitaxially grown but twinned. The degree of twinning can be measured by comparing the thin film azimuthal pole figure intensity data aligned with the substrate direction (A alignment) and 180 degrees from the substrate direction (B alignment). Thin films can also be observed to have random in-plane orientation which would indicate that a film has a fiber texture. It is possible for thin films to exhibit a combination of these in-plane textures. In the case of electro-optic thin films such as LiTaO<sub>3</sub> deposited on  $\alpha$ -Al<sub>2</sub>O<sub>3</sub>, it is important for the LiTaO<sub>3</sub> to be aligned with the substrate to maximize light propagation.

In this paper, we report on the preparation of LiTaO<sub>3</sub>/MgO/Pt deposited on (0001) planar oriented sapphire and the characterization of this multilayer sample using X-ray diffraction techniques.

## Experimental

Sapphire (Union Carbide) single crystal wafers with (0001) orientation were utilized as the substrate for all heteroepitaxial structures in this study. High purity Pt (Johnson Matthey) was deposited on sapphire using electron-beam (e-beam) evaporation. The deposition temperature was 500°C, vacuum was  $3 \times 10^{-8}$  torr, and the deposition rate was 0.5-1.5 Å/s. The final platinum film thickness was ~400 Å. High purity MgO (Aldrich) was then deposited using e-beam evaporation under the same conditions as the initial Pt film with a final MgO film thickness of ~5000 Å. A layer of LiTaO<sub>3</sub> with a thickness of ~2500 Å was deposited on the MgO using laser ablation at a deposition temperature of 650°C. The laser beam was focused onto a target material comprised of polycrystalline LiTaO<sub>3</sub> (Aldrich) with some additional (5 wt.%) polycrystalline Li<sub>2</sub>O (Aldrich). The laser

was a KrF excimer laser operated at a laser pulse energy of 360 mJ with a 30 ns duration and a pulse rate of 4 Hz. The deposition was carried out at a rate of 10 Å/pulse under an oxygen pressure of 92 mtorr. After 250 pulses, the sample was cooled to room temperature in oxygen at a pressure of 150 torr. After fabrication, these heteroepitaxial structures were characterized by XRD without any additional sample preparation.

X-ray diffraction data were collected using a Rigaku RU-300 diffraction system equipped with a thin-film diffractometer and a pole-figure goniometer. Conventional  $\theta/2\theta$  scans were collected utilizing the following parameters:

Goniometer:	horizontal Bragg-Brentano
Radiation:	copper
Monochromator:	diffracted beam flat graphite tuned to CuK $\alpha$
Detector:	scintillation
Slits:	I-1/2° divergence, II-1° scatter, III-0.3 mm receiving, IV-0.6 mm detector
Soller slits:	horizontal used after slit I, parallel between slits II and III
Scan type:	$\theta/2\theta$ coupled
Scan range:	5-70° 2 $\theta$
Step size:	0.01° 2 $\theta$
Count time:	2 s/step

Phase identification and qualitative planar orientation were evaluated using the Powder Diffraction File [7].

Planar orientation was quantitated for the thin films using rocking curve analysis. With the diffractometer mentioned above, samples were scanned across  $\theta$  ( $\omega$ scan) while the detector was held fixed at  $2\theta$ . The  $2\theta$  was predetermined using the  $\theta/2\theta$  coupled scan above. For this diffractometer a single crystal silicon wafer has a rocking curve full width at half maximum (FWHM) of 0.20°  $\theta$ .

To evaluate in-plane orientation of these thin films relative to the sapphire substrate, pole figures were collected utilizing the following conditions:

Goniometer:	Rigaku pole-figure goniometer
Pole figure method:	Schultz reflection mode [8]
Radiation:	copper
Filter	diffracted beam nickel foil
Detector:	scintillation
Slits:	1.2 mm height limiting, 1/2° divergence, Schultz, 1° scatter, 4 mm detector
Scan type:	$\alpha'$ tilt followed by $\beta$ azimuth rotation
Step size:	0.1° $\alpha'$ , 0.1° $\beta$
Count time:	5 s/step
Data correction:	background and absorption

Pole figure tilting is referred to  $\alpha$  (transmission mode) or  $\alpha'$  (reflection mode) on this Rigaku instrument with  $\alpha'=90$  located at the pole figure center. In some instances, pole figure users refer to the tilt axis in a pole figure as  $\phi$  where  $\phi=90-\alpha$  (or  $90-\alpha'$ ). The ability to perform 0.1°  $\alpha'$  and  $\beta$  steps with this pole-figure goniometer is possible with a program written for our laboratory by John Cussen of Rigaku/USA.

Determination of which lattice plane and tilt angle to collect pole-figure data, for each thin film layer as well as the sapphire substrate, was based on the crystal symmetry, lattice constants, and planar orientation of each phase. For LiTaO<sub>3</sub> the (01 $\bar{1}2$ ) plane ( $\alpha'=33.0^\circ$ ), for MgO the (200) plane ( $\alpha'=45.0^\circ$ ), for Pt the (200) plane ( $\alpha'=45.0^\circ$ ) and for  $\alpha$ -Al<sub>2</sub>O<sub>3</sub> the (01 $\bar{1}2$ ) plane ( $\alpha'=32.4^\circ$ ) were selected, respectively.

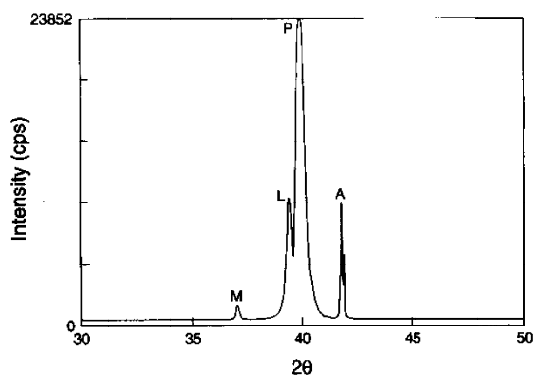


**Fig 1** Selected range diffraction pattern for LiTaO<sub>3</sub>/MgO/Pt(0001)  $\alpha$ -Al<sub>2</sub>O<sub>3</sub> multilayer sample (M-(111) MgO, L-(0006) LiTaO<sub>3</sub>, P-(111)Pt, A-(0006)  $\alpha$ -Al<sub>2</sub>O<sub>3</sub>).

## Results

In Fig. 1, the  $\theta/2\theta$  diffraction pattern for the LiTaO<sub>3</sub>/MgO/Pt/ $\alpha$ -Al<sub>2</sub>O<sub>3</sub> structure is shown. This diffraction pattern is characterized by the presence of (0006) LiTaO<sub>3</sub>, (111) MgO, (111) Pt, and (0006)  $\alpha$ -Al<sub>2</sub>O<sub>3</sub>. No additional diffraction peaks were observed. The rocking curve FWHM values in Table 1 indicate that the planar orientation is very good for all film layers. The quality of the LiTaO<sub>3</sub> film planar orientation was also verified by ion channeling analysis which observed a channeling minimum yield of about 0.25.

The planar orientation revealed in Fig. 1, should result in three-fold symmetry pole figure patterns for the LiTaO<sub>3</sub>, MgO, Pt, and  $\alpha$ -Al<sub>2</sub>O<sub>3</sub> components of this heteroepitaxial structure, assuming that each component is epitaxially aligned with no twinning. This proposed threefold symmetry is a consequence of the crystal lattice type and the planar orientation of each phase. In the case of LiTaO<sub>3</sub> and  $\alpha$ -Al<sub>2</sub>O<sub>3</sub>, (0001) planar orientation (based on hexagonal

**Table 1** X-ray diffraction data for LiTaO<sub>3</sub>/MgO/Pt(0001)  $\alpha$ -Al<sub>2</sub>O<sub>3</sub>

Phase	Lattice type	Planar orientation	Rocking curve FWHM (°)
LiTaO <sub>3</sub>	Trigonal	(0001)	0.83
MgO	Cubic	(111)	0.51
Pt	Cubic	(111)	0.40
$\alpha$ -Al <sub>2</sub> O <sub>3</sub>	Trigonal	(0001)	0.20

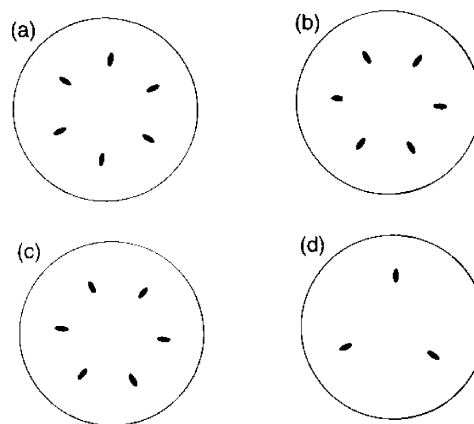


**Fig. 2** Pole figures for LiTaO<sub>3</sub>/MgO/Pt(0001)  $\alpha$ -Al<sub>2</sub>O<sub>3</sub> multilayer sample: (a) (01 $\bar{1}2$ ) LiTaO<sub>3</sub>, (b) (200) MgO, (c) (200) Pt, (d) (01 $\bar{1}2$ )  $\alpha$ -Al<sub>2</sub>O<sub>3</sub>.

indexing), is equivalent to (111) planar orientation when indexed on the true trigonal symmetry of these two phases. In the case of MgO and Pt, the observed planar orientation is cubic (111). Pole figures in Fig. 2 reveal good in-plane alignment but all films are highly twinned. The pole figure for sapphire, Fig. 2(d), shows the expected three pole densities whereas LiTaO<sub>3</sub>, Fig. 2(a), MgO, Fig. 2(b), and Pt, Fig. 2(c) show six pole

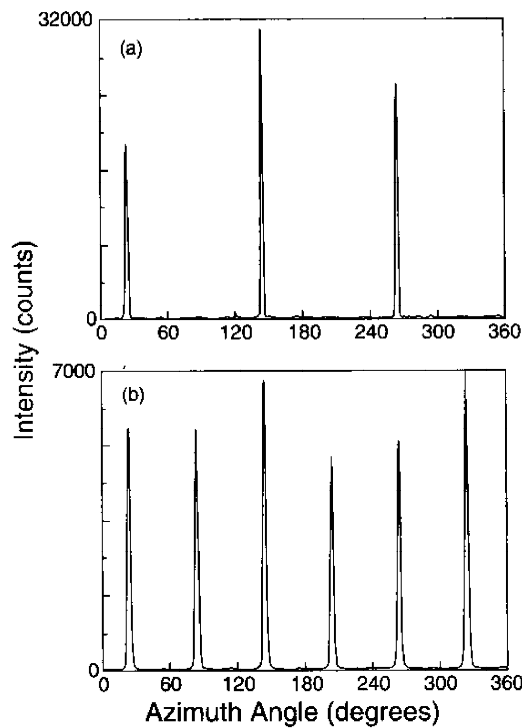


**Fig. 3** Azimuth angle vs. Intensity for (a)  $(01\bar{1}2)$   $\alpha$ -Al<sub>2</sub>O<sub>3</sub> at a tilt angle of 32.4° and (b)  $(01\bar{1}2)$  LiTaO<sub>3</sub> at a tilt angle of 33.0°. Azimuth plot data obtained from pole figures in Fig. 2.

densities each indicative of in-plane twinning. As seen in Fig. 3, a plot of intensity versus azimuth angle reveals that LiTaO<sub>3</sub> is equally aligned with the sapphire substrate, A alignment, and 180° rotated from the wafer, B alignment (Note that the azimuth intensities vary for this sample. This variability is due to the 0.1° azimuth step size which is the minimum step size on the pole figure instrument used in this study. For highly crystalline, high quality epitaxial thin films a 0.01° azimuth step size is necessary for a more accurate assessment of total intensity). Based on the pole density alignment for each phase, the in-plane epitaxial relationships can be determined by referring to stereographic projections [91 and by studying 2-dimensional maps of atomic positions. In Fig. 4, the (0001)  $\alpha$ -Al<sub>2</sub>O<sub>3</sub>, and (111) Pt lattice plane maps are shown to illustrate where atom overlap can occur. The aluminum and platinum atoms have a similar framework which allows epitaxial growth to take place. When deposited on  $\alpha$ -Al<sub>2</sub>O<sub>3</sub> the Pt atoms can be arranged such that the Pt [101] direction is aligned with  $\alpha$ -Al<sub>2</sub>O<sub>3</sub> [ $\bar{1}100$ ] A alignment (Al(+) above the (0001) plane) or [1100] (Al(-) below the (0001) plane) which is the reason twinning is observed in the Pt layer. As a result of the Pt film being twinned, MgO can grow twinned, followed by LiTaO<sub>3</sub> which can grow twinned on MgO. Combining the planar and in-plane orientation results, the complete epitaxial relationship of this heteroepitaxial structure is found to be (0001)[1100] LiTaO<sub>3</sub>/(111)[110] MgO/(111)[110] Pt/(0001) [1100]  $\alpha$ -Al<sub>2</sub>O<sub>3</sub>.

Optical propagation loss (OPL) is used as a measure of the usefulness of a device for electro-

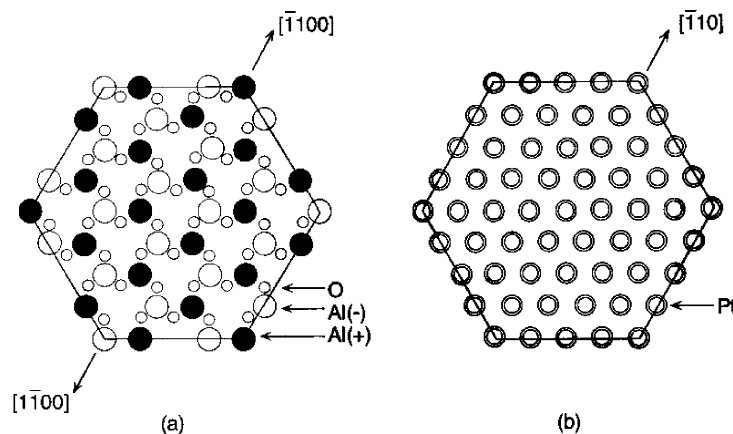


**Fig. 4** Top view of (a) (0001)  $\alpha$ -Al<sub>2</sub>O<sub>3</sub> and (b) (111) Pt planes, showing the in-plane alignment of [1000]  $\alpha$ -Al<sub>2</sub>O<sub>3</sub> and [110] Pt (Al(+) above the (0001) plane, Al(-) below the (0001) plane).

optical devices. For the  $\text{LiTaO}_3/\text{MgO}/\text{Pt}/\alpha\text{-Al}_2\text{O}_3$  device described here, the measured loss was 24 dB/cm. To be acceptable for practical applications, the OPL should be  $< 1$  dB/cm. Additional deposition studies found that depositing thicker films of  $\text{LiTaO}_3$  and  $\text{MgO}$  along with a thinner film of  $\text{Pt}$  did result in some reduction in OPL. However, these changes in deposition resulted in peeling and cracking of the films. A careful study revealed that peeling was attributed primarily to poor adherence of  $\text{Pt}$  to  $\alpha\text{-Al}_2\text{O}_3$  and cracking was partially due to the substantially larger thermal expansion of  $\text{LiTaO}_3$  when compared to  $\alpha\text{-Al}_2\text{O}_3$ . Current studies are looking into replacing  $\alpha\text{-Al}_2\text{O}_3$  with  $\text{LiNbO}_3$  and using a thin  $\text{Ti}$  (titanium) film ( $\sim 40 \text{ \AA}$ ) as an adhesion layer between the  $\text{LiNbO}_3$  substrate and  $\text{Pt}$ .

### Conclusion

Heteroepitaxial structures comprised of  $\text{LiTaO}_3/\text{MgO}/\text{Pt}/\alpha\text{-Al}_2\text{O}_3$  have been fabricated using e-beam and laser ablation deposition techniques. X-ray diffraction methods have been shown to be important in understanding microstructural properties in these structures. Highly oriented crystalline films were obtained which have been demonstrated to function as waveguides. However, high optical propagation losses and film integrity problems were experienced which will require more materials

development before these structures can be used in electro-optical applications.

### Acknowledgments

The authors wish to thank Mr. Craig Barnes for his technical assistance in collecting X-ray diffraction data presented in this publication.

### References

- [1] D. H. Jundt, G. A. Magel, M. M. Fejer, and R. L. Byer, *Appl. Phys. Lett.* **59**, 2657 (1991).
- [2] R. S. Weis and T. K. Gaylord, *Appl. Phys. A* **37**, 191 (1985).
- [3] S. C. Abrahams, J. M. Reddy, and J. L. Bernstein, *J. Phys. Chem. Solids* **27**, 997 (1966).
- [4] J. A. Agostinelli, G. H. Braunstein, T. N. Blanton, *Appl. Phys. Lett.* **63**, 123 (1993).
- [5] A. A. Wernberg, G. Braunstein, G. Paz-Pujait, H. J. Gysling, T. N. Blanton, *Appl. Phys. Lett.* **63**, 331 (1993).
- [6] L. S. Hung, J. A. Agostinelli, J. M. Mir, *Appl. Phys. Lett.* **62**, 3071 (1993).
- [7] Powder Diffraction File, International Centre for Diffraction Data, Newtown Square Corporate Campus, 12 Campus Boulevard, Newtown Square, PA 190733273, USA.
- [8] B. D. Cullity, *Elements of X-ray Diffraction*, AddisonWesley Publishing Co., Reading Mass. (1978).
- [9] E. A. Wood, *Crystal Orientation Manual*, Columbia University Press, New York (1963).

